Quest Journals
Journal of Research in Applied Mathematics
Volume 11 ~ Issue 12 (December 2025) pp: 184-200
ISSN (Online): 2394-0743 ISSN (Print): 2394-0735
www.questjournals.org

Research Paper

Nonlinear Analysis, Stability, and Bifurcation in a Compound Pendulum Model: An Analytical and Numerical Study

Adel Ahmed Hassan Kubba[(1)]
OMER SALEH IBRAHIM MAHMOUD [(2)]
[(1)] *Associate Professor - Nile Valley University - Faculty of Education*
[(2)] *Student*

Abstract
This study presents a comparative investigation into the efficacy of analytical approximation methods for solving the governing equation of a strongly nonlinear, vertically excited pendulum. The pendulum's suspension point is driven by a crank-shaft-slider mechanism (CSSM), leading to a complex nonlinear ordinary differential equation. The primary objective is to obtain accurate approximate solutions for large oscillation amplitudes, where classical perturbation techniques fail. We employ and refine the Modified Harmonic Balance Method (MHBM) and apply He's Frequency Formulation (HFF) method to the derived model. The approximate periodic solutions and system frequencies obtained from these methods are rigorously compared against numerical solutions generated by the fourth-order Runge-Kutta (RK4) method, which serves as a benchmark. Furthermore, a comparison with He's Perturbation Method (HPM) is included. Results demonstrate that the proposed MHBM yields superior accuracy in both displacement solutions and period estimation across a wide range of amplitudes, including extreme cases up to $A = \pi/2$*. The error analysis reveals that the MHBM achieves a significantly lower absolute percentage error (2.34%) in the estimated period for large amplitudes compared to HFF and classical harmonic balance. The study concludes that the MHBM is a robust and highly effective analytical tool for strongly nonlinear oscillators like the excited pendulum model considered.*
Keywords: *Nonlinear pendulum, Modified Harmonic Balance Method (MHBM), He's Frequency Formulation (HFF), Analytical approximation methods, Strongly nonlinear oscillator, Crank-shaft-slider mechanism (CSSM), Periodic solutions, Error analysis, Runge-Kutta method (RK4).*

*Received 15 Dec., 2025; **R**evised 28 Dec., 2025; **A**ccepted 31 Dec., 2025 © The author(s) 2025.*
P**ublished with open access at **www.questjournas.org

I. Introduction

Many manufactured structures incorporate different types of pendulums. To understand the oscillatory motion and basics of mechanics, the study of the simple pendulums plays an important role. The deflection of the simple pendulum is bounded within a very small angle to avoid the nonlinear oscillatory motion. But in the actual situation, the governing equation for the pendulum is nonlinear differential equation. Many researchers contributed to the development of different types of pendulums; for example, Lee and Park studied the chaotic dynamics of a harmonically excited spring-pendulum system with internal resonance, Awrejcewicz, Starosta, and Sypniewska-Kaminska investigated the model of non-´ linear spring subjected to the action of two external forces, Galal et al. studied about the dynamical analysis of a vertical excited pendulum, and so on.[1]

Different types of pendulums are modeled by nonlinear ordinary differential equations, and exact solutions of these equations are rarely found. From last few decades, many researchers developed different methods to deal with the nonlinear oscillators. The perturbation method was used by many researchers earlier and was able to handle only weak nonlinear oscillators. Later, many analytical approximation methods were developed to find approximate solution of the nonlinear oscillators such as the harmonic balance method (HBM), the energy balance method, He's frequency formulation (HFF) method, the homotopy perturbation method, the iteration perturbation method, the max–min approach, and the VIM-Pade technique.[2]

II. Modified Harmonic Balance Method (MHBM)

Let us consider a strongly nonlinear oscillator

$$\ddot{\alpha} + \omega_0^2 \alpha + f(\alpha) = 0, \quad \alpha(0) = A, \ \dot{\alpha}(0) = 0, \tag{1}$$

The function f(α) is nonlinear, satisfying f(−α) = − f(α), with $\omega_0 \geq 0$ (as defined in Table(2.1). The over dots represent derivatives with respect to t

In general, the nth order approximate solution of equation (1) has been found in of the form

$$\alpha(t) = A((1 - u - v - \ldots)\cos \omega t + u \cos 3\omega t + v \cos 5\omega t + \cdots), \tag{2}$$

where u, v, . . . are unknown parameters depending on the amplitude of the oscillator and to be determined and ω is frequency of the oscillator. The zeroth-order approximate solution of equation (1) is obtained by choosing u = v =…= 0, which is

$$\alpha_0(t) \ \ A \cos \omega t. \tag{3}$$

To present the modified form of HBM for higher-order approximate solution, equation (1) can be rewritten as

$$\frac{\ddot{\alpha} + \omega_0^2 \alpha + f(\alpha)}{1 + \alpha_0^2} = 0. \tag{4}$$

Equation (4) can be expanded in a Fourier series as

$$\frac{\ddot{\alpha} + \omega_0^2 \alpha + f(\alpha)}{1 + \alpha_0^2} = k_1(\omega, u, v, \cdots)\cos \omega t + k_3(\omega, u, v, \ldots)\cos 3\omega t + k_5(\omega, u, v, \cdots)\cos 5\omega t + \cdots, \tag{5}$$

where α(t) and $\alpha_0(t)$ are given by equations (2) and (3), respectively, and

$$k_{2n-1}(\omega, u, v, \ldots) = \frac{4}{\pi}\int_0^{\pi/2}\left(\frac{\ddot{\alpha} + \omega_0^2 \alpha + f(\alpha)}{1 + \alpha_0^2}\right)\cos(2n-1)\omega t \, dt, \quad n = 1, 2, \ldots \tag{6}$$

Equations (3.3.4) and (3.3.5) provide

$$k_1(\omega, u, v, \ldots)\cos \omega t + k_3(\omega, u, v, \ldots)\cos 3\omega t + k_5(\omega, u, v, \ldots)\cos 5\omega t + \cdots = 0. \tag{7}$$

Equating the coefficients of like harmonic terms from both sides of equation(7), a system of nonlinear algebraic equations is formed, involving the unknown parameters u, v, … and the unknown angular frequency ω, are obtained. Ignoring the higher-order terms of u, v, … and solving these algebraic equations, the values of u, v, … along with frequency ω can be found.

In particular, the first approximate solution is

$$\alpha(t) = A((1 - u)\cos \omega_t + u \cos 3\omega_t). \tag{8}$$

Now substituting the values of α and α_0 from equations (8) and (3), respectively, in equation (5) and then expanding the resulting equation in a Fourier series and ignoring the higher harmonic terms (more than third harmonic) provides

$$\frac{\ddot{\alpha} + \omega_0^2 \alpha + f(\alpha)}{1 + \alpha_0^2} = k_1(\omega, u)\cos \omega t + k_3(\omega, u)\cos 3\omega t. \tag{9}$$

From equations (4) and (9), the obtained equation is

$$k_1(\omega, u) \cos \omega t + k_3(\omega, u) \cos 3\omega t = 0. \quad (10)$$

Equating the coefficients of cos ωt and cos 3ωt from both sides of equation (10), it gives

$$k_1(\omega, u) = 0, \quad (11)$$

$$k_3(\omega, u) = 0. \quad (12)$$

Ignoring the higher-order terms of u and solving above equations, the values of u and ω can be found. So the first approximation solution is

$$\alpha(t) = A((1 - u) \cos \omega t + u \cos 3\omega t), \quad (13)$$

where u and ω are the solutions of equations (11) and (12).[3]

Table 2.1: Nomenclature.

Nomenclature	The meaning
A	Amplitude of the oscillator
α_{nu}	Runge–Kutta fourth-order method solution
α_{MHBM}	Modified harmonic balance method solution
α_{HPM}	He's perturbation method solution
α_{HFF}	He's frequency formulation method solution
ω_0	Natural frequency
ω	Frequency of the oscillator
$u, v, \ldots$	Unknown parameters for the MHBM
$k_1(\omega, u, v, \ldots), k_3(\omega, u, v, \ldots), \ldots$	Fourier series coefficients
HFF	He's frequency formulation
HPM	He's perturbation method
MHBM	Modified harmonic balance method
t	Time
ω_{nu}	Frequency obtained by the Runge–Kutta fourth-order method
ω_{MHBM}	Frequency obtained by the modified harmonic balance method
ω_{HFF}	Frequency obtained by He's frequency formulation method

III. The Solution of Vertical Excited Pendulum

Modified Harmonic Balance Solution (3.1)[4] Let us presume that the pendulum's point of suspension undergoes vertical motion through the CSSM as depicted in Figure 3.1. The system comprises a rigid, weightless rod of length l, connected at one end to a mass m. This mass experiences vertical excitation via the CSSM. Additionally, a weightless rod of length a rotates at a constant angular velocity while a link b facilitates vertical movement of the pendulum's suspension point. In essence, the pendulum features a single mass m situated at its extremity.

Let α denote the rotation angle of the pendulum, representing its generalized coordinate. In order to formulate the Lagrange's function for the system, the coordinates of the mass can be expressed as

$$x = l \sin \alpha, \quad (14)$$

$$y = -a \cos \theta - b \cos \phi - l \cos \alpha,$$

where θ and ϕ represent the angles between OB and OA and OB and BA, respectively, as illustrated in Figure 3.1. Utilizing the trigonometric relationship between θ and ϕ, one can express cos ϕ as

$$\cos \phi = \left(1 - \frac{a^2}{b^2} \sin^2 \theta\right). \quad (15)$$

Combining equations (14) and (15), the first derivative with respect to time t can be expressed as follows:

(16)

$$\dot{y} = a\dot{\theta}\sin\theta + \frac{a^2\dot{\theta}\sin\theta\cos\theta}{b\left(1-\left(a^2/b^2\right)\sin^2\theta\right)^{(1/2)}} + l\dot{\alpha}\sin\alpha.$$

Introducing a dimensionless variable F′ which depends on θ, we write:

(17)

$$F' = \sin\theta + \frac{a\sin\theta\cos\theta}{b\left(1-a^2/b^2\sin^2\theta\right)^{(1/2)}}.$$

Substituting equations (17) into (16), it becomes

(18)

$$\dot{x} = l\dot{\alpha}\cos\alpha,$$

$$\dot{y} = a\dot{\theta}F' + l\dot{\alpha}\sin\alpha.$$

The kinetic energy T and potential energy V can be computed using the provided information in the following manner:

$$T = \frac{1}{2}m\left(l^2\dot{\alpha}^2\cos^2\alpha + \left(a\dot{\theta}F' + l\dot{\alpha}\sin\alpha\right)^2\right),$$

(19)

$$V = -mgl\cos\alpha - mgb\left(1-\frac{a^2}{b^2}\sin^2\theta\right)^{(1/2)} - mga\cos\theta,$$

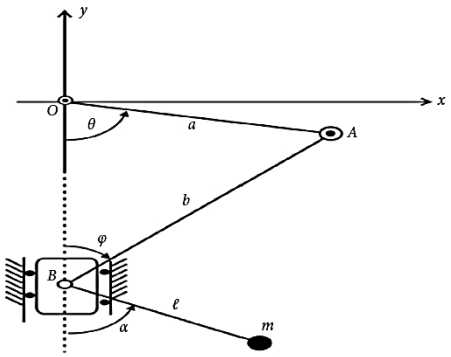

Figure 3.1: The dynamical model for the excited pendulum by a crank-shaft-slider mechanism (CSSM)

where g represents gravitational acceleration and dots denote derivatives with respect to time, t. Lagrange's equation for the conservative system under consideration takes the form

(20)

$$\frac{\mathrm{d}}{\mathrm{d}t}\left(\frac{\partial L}{\partial\dot{\alpha}}\right) - \left(\frac{\partial L}{\partial\alpha}\right) = G_{\alpha}^{\mathrm{NC}} = -cl^2\dot{\alpha},$$

where L = T − V and $G^{NC}{}_{\alpha}$ represent the generalized force which has a dimension of moment and c is the coefficient of friction. Hence, the EOM may be reduced to

(21)

$$ml\ddot{\alpha} + ma\dot{\theta}F'\sin\alpha + mg\sin\alpha = -cl\dot{\alpha}.$$

Introducing dimensionless time τ, then according to the transformation

$\tau\ \omega_0 t$, where $\omega_0 = \sqrt{g/l}$, we can write

$$\dot{\alpha} = \omega_0 \alpha', \ \ddot{\alpha} = \omega_0^2 \alpha'', \ F' = \omega_0 F, \ \dot{\theta} = \omega_0 \theta' = \omega_0 \Omega.$$

Using the above relations, the equation of motion of an excited pendulum formulated with the assumption that its suspension point moves vertically and is supported by the CSSM becomes

$$\ddot{\alpha} + \left(1 + \frac{a}{l}\Omega F\right) \sin\alpha = 0, \tag{22}$$

where Ω and F are the dimensionless variables depending on the angle θ.

For convenience, equation (22) can be represented as

$$\alpha'' + k \sin\alpha = 0, \tag{23}$$

where $k(1+(a/l)\Omega F)$ is an arbitrary constant when ΩF is assumed as a constant and the initial conditions are given as $\alpha(0)$ A, $\dot{\alpha}(0) = 0$. Taylor's series expansion provides $\sin\alpha = \alpha - (\alpha^3/3!) + (\alpha^5/5!) - \ldots$ Considering the terms up to α^5 of sin α series, equation (23) is then reduced to

$$\ddot{\alpha} + k\left(\alpha - \frac{\alpha^3}{3!} + \frac{\alpha^5}{5!}\right) = 0. \tag{24}$$

According to the present modified method, equation (24) can be written as

$$\frac{\ddot{\alpha} + k\left(\alpha - \left(\alpha^3/3!\right) + \left(\alpha^5/5!\right)\right)}{1 + \alpha_0^2} = 0. \tag{25}$$

Using the values of $\alpha_0(t)$ and $\alpha(t)$ from equations (3) and (8), respectively, in equation (25) and expanding in a Fourier series up to third harmonic terms, the equation becomes

$$\frac{\ddot{\alpha} + k\left(\alpha - \left(\alpha^3/3!\right) + \left(\alpha^5/5!\right)\right)}{1 + \alpha_0^2} = k_1(\omega, u)\cos\omega t + k_3(\omega, u)\cos 3\omega t, \tag{26}$$

where $k_1(\omega, u) = b_1 + b_2\omega_2 + (b_3 + b_4\omega^2)u + O(u^2)$,
$k_3(\omega, u) = d_1 + d_2\omega^2 + (d_3 + d_4\omega^2)u + d_5 u^2 + O(u^3)$, (27)

and

$$b_1 = \left(\frac{47k}{20A}\right) - \frac{7Ak}{40} + \frac{A^3k}{160} - \frac{47k}{20A\sqrt{1+A^2}},$$

$$b_2 = -\frac{2}{A} + \frac{2}{A\sqrt{1+A^2}},$$

$$b_3 = -\left(\frac{37k}{3A^3}\right) - \left(\frac{37k}{6A}\right) + \frac{13Ak}{24} - \frac{A^3k}{48} + \frac{37k}{3A^3\sqrt{1+A^2}} + \frac{37k}{3A\sqrt{1+A^2}},$$

$$b_4 = \frac{72}{A^3} + \frac{20}{A} - \frac{72}{A^3\sqrt{1+A^2}} - \frac{56}{A\sqrt{1+A^2}},$$

$$d_1 = -\left(\frac{47k}{5A^3}\right) - \left(\frac{47k}{20A}\right) + \frac{A^3k}{480} + \frac{47k}{5A^3\sqrt{1+A^2}} + \frac{141k}{20A\sqrt{1+A^2}},$$

$$d_2 = \frac{8}{A^3} + \frac{2}{A} - \frac{8}{A^3\sqrt{1+A^2}} - \frac{6}{A\sqrt{1+A^2}},$$

$$d_3 = \left(\frac{148k}{3A^5}\right) + \left(\frac{185k}{3A^3}\right) + \left(\frac{37k}{3A}\right) - \frac{13Ak}{24} + \frac{A^3k}{96} - \frac{148k}{3A^5\sqrt{1+A^2}} - \frac{259k}{3A^3\sqrt{1+A^2}} - \frac{37k}{A\sqrt{1+A^2}},$$

$$d_4 = -\frac{288}{A^5} - \frac{296}{A^3} - \frac{56}{A} + \frac{288}{A^5\sqrt{1+A^2}} + \frac{440}{A^3\sqrt{1+A^2}} + \frac{168}{A\sqrt{1+A^2}},$$

$$d_5 = -\left(\frac{224k}{3A^7}\right) - \frac{168k}{A^5} - \frac{112k}{A^3} - \left(\frac{49k}{3A}\right) + \frac{7Ak}{4} - \frac{A^3k}{16} + \frac{224k}{3A^7\sqrt{1+A^2}} + \frac{616k}{3A^5\sqrt{1+A^2}} + \frac{560k}{3A^3\sqrt{1+A^2}} + \frac{56k}{A\sqrt{1+A^2}}. \quad (28)$$

Equations (25) and (26) provide

$$k_1(\omega, u)\cos\omega t + k_3(\omega, u)\cos 3\omega t = 0. \quad (29)$$

Using equations (27) in (29) and ignoring the higher-order terms of u and equating the coefficient of cos ω_t and cos $3\omega_t$ from both sides, it gives

$$b_1 + b_2\omega^2 + (b_3 + b_4\omega^2)u = 0, \quad (30)$$

$$d_1 + d_2\omega_2 + (d_3 + d_4\omega^2)u + d_5 u^2 = 0. \quad (31)$$

Eliminating ω^2 from equations (30) and (31) and solving for u, it provides

$$u = \frac{-l_1 + \sqrt{l_1^2 - 4l_0l_2}}{2l_2}, \quad (32)$$

where

$$l_0 = -b_1d_1,$$
$$l_1 = -b_3d_1 + b_2d_2 - b_1d_3, \quad (33)$$
$$l_2 = -b_5d_1 + b_4d_2 - b_3d_3 + b_2d_4.$$

Solving equation (30) for ω, it gives

$$\omega = \frac{\sqrt{-b_1 - b_3u}}{\sqrt{b_2 + b_4u}}. \quad (34)$$

So the first approximation solution of equation (23) is

$$\alpha(t) = A((1-u)\cos\omega t + u\cos 3\omega t), \tag{35}$$

where u and ω are given by equations (3.3.32) and (3.3.34), respectively.

IV. HFF Method Solution. According to HFF method,

considering the two trial solutions $\alpha_1 = A\cos\omega_1 t$ and $\alpha_2 = A\cos\omega_2 t$ for equation (23), the two obtained residuals are as

$$R_1(t) = \frac{1}{120}\left(120\left(k-\omega_1^2\right)A\cos\omega_1 t - 20A^2k\cos^2\omega_1 t + A^4k\cos^4\omega_1 t\right), \tag{36}$$

$$R_2(t) = \frac{1}{120}\left(120\left(k-\omega_2^2\right)A\cos\omega_2 t - 20A^2k\cos^2\omega_2 t + A^4k\cos^4\omega_2 t\right). \tag{37}$$

$$\tilde{R}_1 = \frac{1}{T}\int_0^T R_1(t)\cos\omega_1 t\,dt \tag{38}$$

$$\tilde{R}_2 = \frac{1}{T}\int_0^T R_2(t)\cos\omega_2 t\,dt = \frac{1}{384}A\left(\left(192-24A^2+A^4\right)k - 192\omega_2^2\right). \tag{39}$$

For the oscillator equation (23), it is found that

$$\omega^2 = \left(\frac{\omega_1^2\tilde{R}_2 - \omega_2^2\tilde{R}_1}{\tilde{R}_2 - \tilde{R}_1}\right) = k\left(1 - \frac{A^2}{8} + \frac{A^4}{192}\right). \tag{40}$$

Hence, the frequency of the oscillator represented by equation (23) is [5]

$$\alpha(t) = A\cos\left(\sqrt{k\left(1-\frac{A^2}{8}+\frac{A^4}{192}\right)}\right)t. \tag{41}$$

V. Method

When solving practical problems, we often encounter nonlinear physical equations. Consider the cubic nonlinear Schrödinger equation, as follows:

$$i\frac{\partial\psi}{\partial t} + \frac{1}{2}\Delta\psi + \kappa|\psi|^2\psi = 0 \tag{42}$$

$$iu_t + u_{xx} + v|u|^2u = 0 \tag{43}$$

To solve its traveling wave solutions, one can set:

$$u(x,t) = e^{i\frac{D}{2}x - i\left(\frac{D^2}{4}-\alpha\right)t}\cdot v(\xi) \tag{44}$$

Where we set $\xi = x - Dt$, and transform the equation (2) into:

$$\ddot{u} - \alpha u - v u^3 = 0 \tag{45}$$

Perform first order integration with respect to ξ, equation (45) is converted to:

(46)

$$\dot{u}^2 = c + \alpha u^2 - \frac{v}{2}u^4$$

The problem of solving the nonlinear equation is transformed into solving equations (45) and (46).
In various fields, there are many other nonlinear physical equations, such as the Beam Propagation equation in nonlinear optics

(47)

$$2ik\frac{\partial \psi}{\partial x} + \nabla_{\perp}^2 \psi + \frac{n_2}{n_1}k^2|\psi|^2\psi$$

The Korte Weg–de Vries equation under the shallow water wave approximation.

$$u_t + uu_x + uu_{xxx} = 0 \tag{48}$$

The Boussinesq-Schrödinger-Gardner (BSG) equation.

$$u_{tt} - u_{xx} - u_{xxxx} + 3(u^2)_{xx} = 0 \tag{49}$$

The sine-Gordon equation and the double sine-Gordon equation in optics:

$$u_{xx} - u_{tt} = \sin u + \frac{1}{3}\sin\frac{u}{2} \tag{50}$$

This type of equations can be transformed into standard form of ϕ^4 equation with different λ and σ value through appropriate transformations.

$$^2\phi = \lambda\phi^3 + \sigma\phi \tag{51}$$

Or it's one dimension form:

$$\phi_{xx} - \phi_{tt} = \lambda\phi^3 + \sigma\phi \tag{52}$$

Solution for the ϕ^4 equation (5.1)[6] For equation (52), when considering its traveling wave form, a new independent variable η is defined, where

(53)

$$\eta = \frac{x - vt}{\sqrt{1 - v^2}}$$

Therefore, transform equation (52) into the form:

$$\phi_{\eta\eta} = \lambda\phi^3 + \sigma\phi \tag{54}$$

The term $\phi_{\eta\eta}$ represents the second order derivative of ϕ with respect to η. By leveraging the relationship with ϕ_η

(55)

$$\phi_{\eta\eta} = \frac{1}{2}\frac{d}{d\phi}\phi_\eta^2$$

Substitute equation (55) into equation (54).

(56)

$$\phi_\eta^2 = \frac{\lambda}{2}\phi^4 + \sigma\phi^2 + c_1$$

Consider different values of λ, σ and c_1, the behavior of the solution of ϕ in equation (56) can be variable. By analyzing the form of the solution, there will be 2 kinds of solution: the periodic solution and solution, the solution solutions always appear with specific λ, σ, c_1 value.

Form of solution when λ< 1 (5.2)[6] Here, a new independent variable ξ is defined, along with a function u(ξ) of it.

$$\xi = \sqrt{\frac{\sigma}{2\alpha}}\eta \tag{57}$$

$$\phi(\eta) = \sqrt{\frac{\sigma}{2\alpha\lambda}}u\left(\sqrt{\frac{\sigma}{2\alpha}}\eta\right) \tag{58}$$

$$u_\xi^2 = -u^4 + 2\alpha u^2 + c \tag{59}$$

Typically, α is taken as:

$$\begin{cases} \sigma > 0, \alpha = +1 \\ \sigma < 0, \alpha = -1 \end{cases}$$

Comparing the equation (56) and equation (59), c in equation (59) is:

$$c = -\frac{4\lambda}{\sigma^2}c_1 \tag{60}$$

Since the λ < 1, c have same sign as c_1, therefore, with different value of c, equation gets different series of solution:

When σ > 0 (5.3)[6] When σ>0, α is+1, for c>0 the solution of equation(59) is:

$$u(\xi) = \pm\frac{\sqrt{c}}{\sqrt{2}(1+c)^{\frac{1}{4}}} \cdot \mathrm{sd}\left(\sqrt{2}(1+c)^{\frac{1}{4}}(\xi - \xi_0); \frac{1+\sqrt{1+c}}{2\sqrt{1+c}}\right) \tag{61}$$

It can be observed that the solution exhibits periodicity under these conditions from figure 7.1.
When c = 0:

$$u(\xi) = \pm \sqrt{2}\ \mathrm{sech}\ (\sqrt{2}\ (\xi - \xi_0)) \tag{62}$$

This time, a solution is obtained in figure 7.2.
When −1 < c < 0:

$$u(\xi) = \pm\sqrt{1+\sqrt{1+c}} \cdot \mathrm{dn}(\sqrt{1+\sqrt{1+c}}(\xi - \xi_0); \frac{2\sqrt{1+c}}{1+\sqrt{1+c}}) \tag{63}$$

As shown in figure 7.3, when σ > 0 and c < 0, the solution of the equation is a traveling wave solution with periodicity, Additionally, compared to the figure 7.1, it can be observed that the solution graph lies above the x-axis (if the coefficient is negative, it lies below the x-axis; here we only consider positive coefficients). This is because the solution includes the Jacobi elliptic function d_n, whose values are always greater than 0. Where $\mathrm{sd}\xi = \frac{\mathrm{sn}\xi}{\mathrm{dn}\xi}$, sdξ, d_n ξ, s_n ξ are all Jacobi elliptic functions.

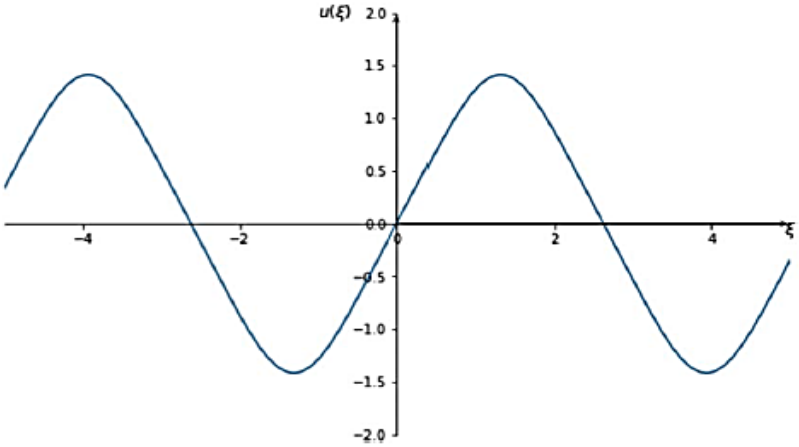

Figure5.1. The traveling wave solution of equation (60) when σ>0 and c>0.

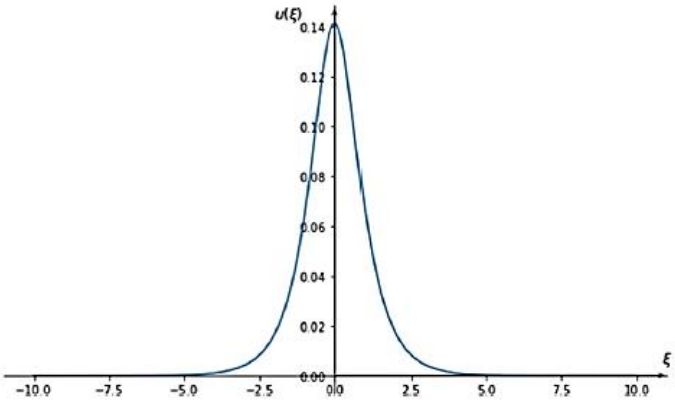

Figure 5.2. Solution of equation (60) when σ > 0 and c = 0.

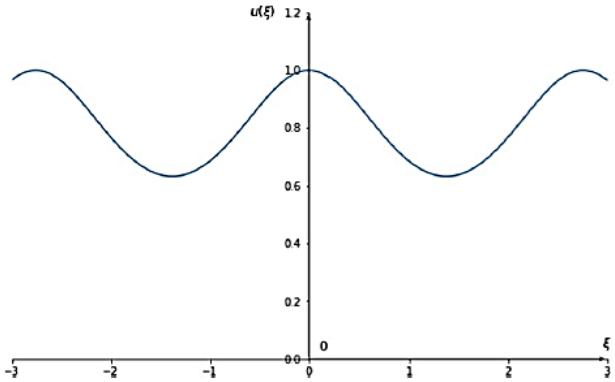

Figure 5.3. Periodic solution of equation (60) when σ > 0 and c < 0.

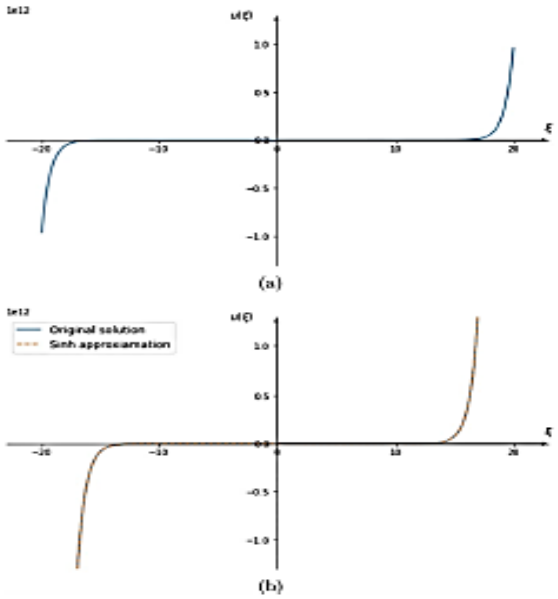

Figure 5.4. (60): the calculation result of equation (60) when $\frac{1+\sqrt{1+c}}{2\sqrt{1+c}} \to 1$, (61): the approximate result of equation (63) compared to the original result of equation (62).

In the situation corresponding to equation (62), when $\frac{1+\sqrt{1+c}}{2\sqrt{1+c}} \to 1$, the equation (60) can be approximated as:

$$u(\xi) \to \pm\frac{\sqrt{c}}{\sqrt{2}(1+c)^{\frac{1}{4}}}\sinh(\sqrt{2}(1+c)^{\frac{1}{4}}(\xi-\xi_0))$$

The function derived at this point loses its periodicity with respect to ξ. For the Sine-Gordon equation, this solution is a typical kink-type soliton solution.

The comparison between the two, as shown in figure 7.4, reveals that the difference between them is minimal.

When $c \le -1$, the equation has no real solutions.

When σ < 0 (5.4)[7] When σ<0, α is −1. Thus, the real solution only exists when $c > 0$:

(64)

$$u(\xi) = \pm\frac{\sqrt{c}}{\sqrt{2}(1+c)^{\frac{1}{4}}} \cdot \mathrm{sd}(\sqrt{2}(1+c)^{\frac{1}{4}}(\xi-\xi_0); \frac{\sqrt{1+c}-1}{2\sqrt{1+c}})$$

As shown in figure 5.5, when $\sigma < 0$ and $c > 0$, this solution is also a traveling wave solution with periodicity, similar to figure 5.1. However, under the same parameters, it has a smaller amplitude and period.

when $c = 0$ we have trivial solution $u(\xi) = 0$. When $c \le 0$, there are exclusively complex solutions.

By substituting equations (60), (62), (63), and (64) into the original equation (64), these solutions satisfy the equation under their respective conditions.

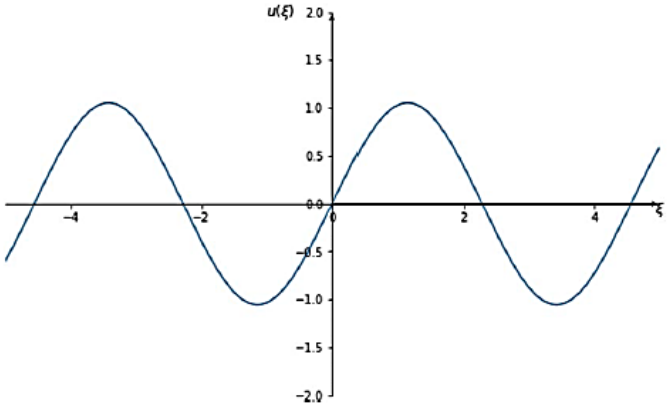

Figure5.5. The traveling wave solution of equation(62) when σ<0 and c>0

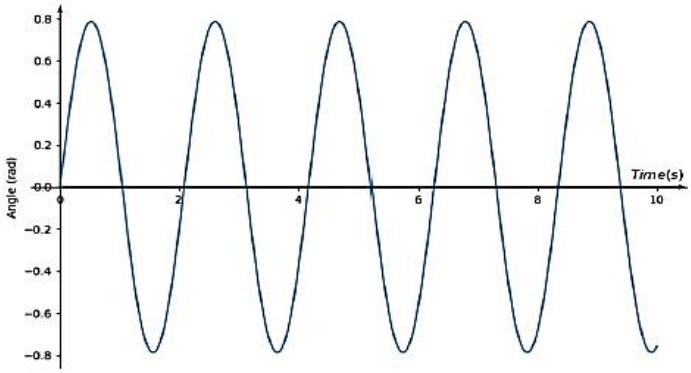

Figure 5.6. The graph derived from equation (22) demonstrates that the solution exhibits periodicity.

VI. Discussion on the simulation of the compound pendulum

The analysis of the solution forms reveals two distinct types: periodic traveling wave solution and soliton solutions. If the physical problem involves damping, solving the corresponding equations and to identify soliton solutions. It will be discussed by using a compound pendulum model below. Consider a compound pendulum in a classical mechanics model. The dynamics equations are as follows:[8]

$$I\ddot{\theta} = -mgl_c \sin\theta \tag{65}$$

Where I is the moment of inertia about the axis, l_c is the distance between center of mass and the axis. Performing a single integration on the given equation yields the energy equation for a compound pendulum.

$$\frac{1}{2}I\dot{\theta}^2 = mgl_c(\cos\theta - \cos\theta_0) \tag{66}$$

and the constant θ_0 is the amplitude of the pendulum. By introducing two new constants, equation (66) can be rearranged as:

$$k\dot{\theta}^2 = \cos\theta - c \tag{67}$$

where $k = \frac{I}{2mgl_c}$, $c = \cos\theta_0$.

Subsequently, define a new variable $u = \tan\frac{\theta}{2}$, express the θ cos and $\dot{\theta}$ in terms of u:

$$\cos(\theta) = \frac{1 - \tan^2\left(\frac{\theta}{2}\right)}{1 + \tan^2\left(\frac{\theta}{2}\right)} = \frac{1 - u^2}{1 + u^2} \tag{68}$$

$$\dot{\theta} = \frac{d}{dt}[2\arctan(u)] = \frac{2\dot{u}}{1 + u^2} \tag{69}$$

Substitute cos θ and $\dot{\theta}$ back into equation (67) and simplify:

$$\dot{u}^2 = \frac{1}{4k}(1 + c)(1 + u^2)\left(\frac{1 - c}{1 + c} - u^2\right) \tag{70}$$

By comparing equation (70) with equation (69), it can be observed that this equation is identical in form to the ϕ^4 equation with $\lambda < 0$, we define a new variable t which represent the time, thus a solution can be obtained.

$$u = \pm\sin\frac{\theta_0}{2} \cdot \mathrm{sd}\left(\frac{t - t_0}{2k}; \sin^2\frac{\theta_0}{2}\right) \tag{71}$$

Based on the relationship between u and θ, the complete mathematical solution to the compound pendulum problem is given by

$$\theta = \pm 2\arctan\left\{\sin\frac{\theta_0}{2}\,\mathrm{sd}\left(\sqrt{\frac{mgl}{I}}(t - t_0); \sin^2\frac{\theta_0}{2}\right)\right\} \tag{72}$$

According to equation (71), the relationship between time and angle should be as shown in figure 6.1.

Example (6.1)[8] Table 8.1 shows the solution of the governing equation for an excited pendulum by a CSSM obtained by Runge–Kutta fourth-order method, He's perturbation method (HPM), HFF method, and MHBM when A = 1.0, a = 1.0, l = 0.75, Ω = 5, F = 0.6. Similarly, Table 3 displays the solution obtained for the pendulum equation by various methods. For both cases with similar conditions and with different lengths of weightless rod a, the present method provides better solution. The comparison among the solutions, presented in Tables 6.2 and 6.3, indicates the supremacy of the MHBM.

Here the error is considered as

$$\text{error\%} = \left|\left(\frac{\text{Exact Value}\left(\text{Runge} - \text{Kutta } 4^{\text{th}} \text{ order solution}\right) - \text{Present value}}{\text{Exact Value}\left(\text{Runge} - \text{Kutta } 4^{\text{th}} \text{ order solution}\right)}\right)\right| \times 100. \tag{73}$$

In Figure 6.2, the solutions for the governing equation (73) obtained by different methods are displayed for the parameters a = 2.0, l = 0.75, Ω = 5, F = 0.6 when amplitude is A = 1.0. From Figure 3.3.2, it is obvious that all solutions show a good agreement with numerical solution except HPM solution. Figure 6.2 also shows that HPM solution diverges after a certain time interval.

In Figures 6.3 and 6.4, the solutions for the governing equation (73) obtained by different methods are displayed for the parameters a = 1.0, l = 0.75, Ω = 5, F = 0.6 and a = 2.0, l = 0.75, Ω = 5, F = 0.6, respectively, when amplitude is

A = π/2. It is worth mentioning that HPM solution] diverges for the amplitude A = π/2. If the length of the rod is longer, then from both figures, it is obvious that the MHBM solution shows better consistency than

HFF solution. Figure 6.5 represents the MHBM solution of the present problem when time and amplitude vary as $0 \le t \le 10.2$ and $0 < A \le 0.5$, respectively, for a = 1.0, l = 0.75, Ω = 5, F = 0.6.
Figure 6.6 represents the MHBM solution of the present problem when time and amplitude vary as $0 \le t \le 10.2$ and $0.5 \le A \le 1.0$, respectively, for a = 1.0, l = 0.75, Ω = 5, F = 0.6. All the figures and tables show the goodness of the MHBM solution over the HFF method and HPM solutions.
The exact period of the pendulum equation (74) is given by

$$T_{ex} = T_0\left(1 + \frac{A^2}{16} + \frac{11A^4}{3072} + \frac{173A^6}{737280} + \frac{22931A^8}{1321205760} + \cdots\cdots\cdots\right), \tag{74}$$

The second approximate period obtained using the HBM and the first approximate period from the HFF method are identical, given by

$$T_{app2} = T_0\left(1 + \frac{A^2}{16} + \frac{10A^4}{3072} + \frac{90A^6}{737280} + \cdots\cdots\cdots\right). \tag{75}$$

Taking terms up to $O(A^6)$, we find that

$$\lim_{A \longrightarrow 180^\circ} \frac{T_{HBM2}}{T_{ex}} = \lim_{A \longrightarrow 180^\circ} \frac{T_{HFF1}}{T_{ex}} \cong 0.936. \tag{76}$$

Table 6.2: Comparison among the solutions of the pendulum model obtained by numerical method (RK4), He's perturbation method, HFF method, and MHBM when A = 1.0, a = 1.0, l = 0.75, Ω = 5, F = 0.6.

Time t	α_{nu}	α_{HPM} error %	α_{HFF} error %	α_{MHBM} error %
0	1.00000	1.00000 0.00	1.00000 0.00	1.00000 0.00
1	−0.510575	−0.511338 0.15	−0.503003 1.48	−0.510713 0.027
2	−0.503852	−0.507769 0.78	−0.493976 1.96	−0.503658 0.039
3	0.999971	1.00744 0.75	0.999945 0.003	0.999969 0.000
4	−0.517265	−0.513899 0.65	−0.511975 1.023	−0.517733 0.09
5	−0.497096	−0.546238 9.89	−0.484896 2.45	−0.496567 0.106
6	0.999886	1.07593 7.61	0.999783 0.01	0.999875 0.001
7	−0.523921	−0.507931 3.05	−0.520891 0.58	−0.524715 0.152
8	−0.490308	−0.656591 33.91	−0.475763 2.97	−0.489440 0.177
9	0.999744	1.2954 29.57	0.999512 0.023	0.999718 0.003
10	−0.530544	−0.584202 10.11	−0.529751 0.149	−0.531660 0.21

Table 6.3: Comparison among the solutions of the pendulum model obtained by numerical method (RK4), He's perturbation method, HFF method, and MHBM when A = 1.0, a = 2.0, l = 0.75, Ω = 5, F = 0.6.

Time t	α_{nu}	α_{HPM} error %	α_{HFF} error %	α_{MHBM} error %
0	1.00000	1.00000 0.00	1.00000 0.00	1.00000 0.00
1	−0.948752	−0.949142 0.04	−0.947007 0.184	−0.948866 0.012
2	0.798638	0.799297 0.08	0.793644 0.625	0.798960 0.04
3	−0.561673	−0.558623 0.54	−0.556167 0.98	−0.562145 0.084
4	0.260424	0.240618 7.61	0.259743 0.26	0.261069 0.25
5	0.0717943	0.136085 89.95	0.0642099 10.564	0.0709214 1.216
6	−0.395393	−0.5481 38.62	−0.381357 3.55	−0.394441 0.24
7	0.672607	0.967936 43.91	0.658086 2.16	0.671817 0.12
8	−0.87448	−1.36496 56.09	−0.865067 1.08	−0.873938 0.062
9	0.983185	1.70674 73.59	0.980363 0.287	0.982935 0.025
10	−0.990557	−1.96069 97.94	−0.991754 0.121	−0.990796 0.024

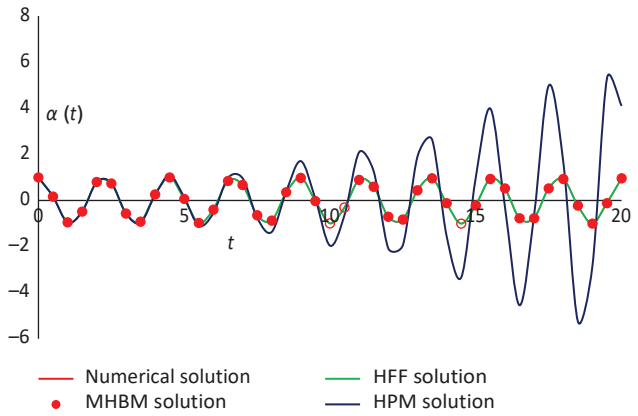

Figure 6.2: Comparison of the pendulum model solution obtained by numerical method (RK4), He's perturbation method, HFF method, and MHBM when
A = 1.0, a = 2.0, l = 0.75, Ω = 5, F = 0.6.

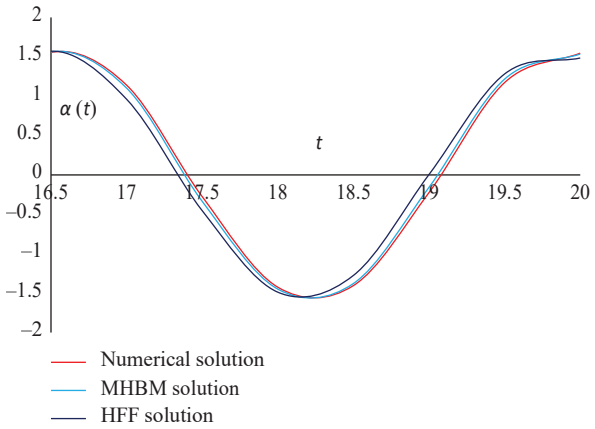

Figure 6.3: Comparison of the pendulum model solutions obtained by numerical method (RK4), HFF method, and MHBM when A= π/2, a =1.0,

l = 0.75, Ω = 5, F = 0.6, and 16.5 ≤ t ≤ 20.

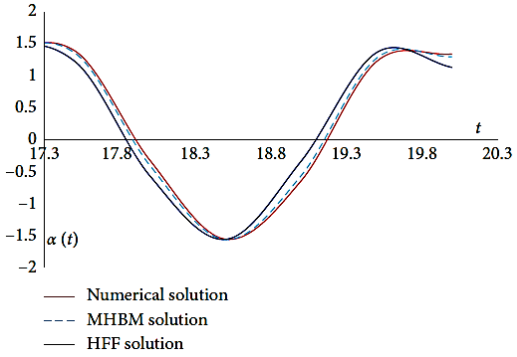

Figure 6.4: Comparison of the pendulum model solutions obtained by numerical method (RK4), HFF method, and MHBM when A = π/2, a = 2,

l = 0.75 , Ω 5, F 0.6, and 17.3 ≤ t ≤ 20.

Thus, the absolute percentage error is 6.39%, w he A ⟶ 180° for any choice of the parameter k(1 + (a/l) ΩF). Therefore, variations in parameters a, l, Ω, and F do not affect the error.

The first approximate period obtained using the present method is

$$T_{\text{app1}} = T_0\left(1 + \frac{A^2}{16} + \frac{11A^4}{3072} + \frac{133.75A^6}{737280} + \cdots\cdots\cdots\right). \tag{77}$$

Taking terms up to $O(A^6)$, we find that for MHBM,

$$\lim_{A \longrightarrow 180^\circ} \frac{T_{\text{MHBM1}}}{T_{ex}} \cong 0.9766.$$

Thus, the absolute percentage error is 2.34% when A ⟶ 180° for any choice of the parameter k(1 + (a/l)ΩF). Therefore, again variations in parameters a, l, Ω, and F do not influence the error.

It is evident that the relative error for the second approximate period from the HBM and the first approximate period from the HFF method is significantly larger than the error obtained using the present method, regardless of the choice of parameters a, l, Ω, and F.

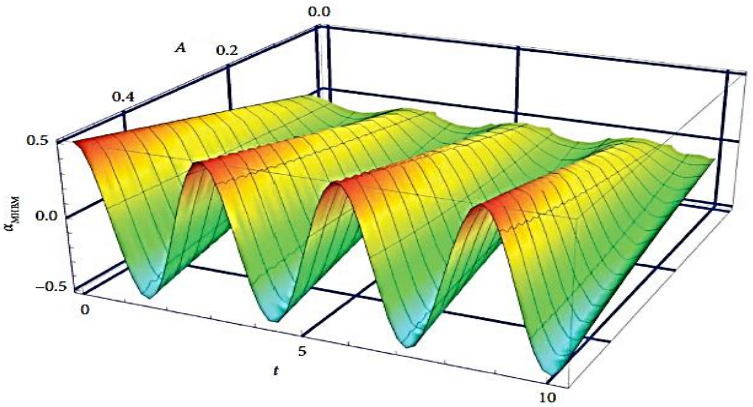

Figure 6.5: Modified harmonic balance method solution when a = 1, l = 0.75 , Ω = 5, F = 0.6, 0 < A ≤ 0.5, and 0 ≤ t ≤ 10.2.

VII. Conclusion

This study summarizes the findings of a comparative analysis of three analytical approximation methods for solving the dynamics of a strongly nonlinear pendulum vertically excited via a crank-shaft-slider mechanism. The results demonstrate a clear superiority of the Modified Harmonic Balance Method (MHBM) in terms of accuracy and stability, particularly at large amplitudes ($A = \pi/2$), where He's Perturbation Method (HPM) failed to converge. The error in the estimated period using MHBM was only 2.34%, compared to 6.39% for other methods, while maintaining high accuracy in modeling displacement over time. These findings confirm the validity of MHBM as an effective and reliable tool for analyzing complex nonlinear oscillatory systems. The paper recommends its adoption for similar dynamical models, as it provides highly accurate harmonic solutions with reasonable computational complexity.

References

[1]. **Lee, W.K., & Park, H.D.** (2022). *Chaotic dynamics of a harmonically excited spring-pendulum system with internal resonance.*
[2]. **Awrejcewicz, J., Starosta, R., & Sypniewska-Kaminska, G.** (2019). *On the model of non-linear spring subjected to the action of two external forces.*
[3]. **Galal, A. et al.** (2012). *Dynamical analysis of a vertical excited pendulum.*
[4]. **He, J.H.** (2002). *Preliminary report on the energy balance for nonlinear oscillations.* Mechanics Research Communications, 29(2), 107-111.
[5]. **He, J.H.** (2006). *Some asymptotic methods for strongly nonlinear equations.* International Journal of Modern Physics B, 20(10), 1141-1199.
[6]. **Mickens, R.E.** (2010). *Truly Nonlinear Oscillations: Harmonic Balance, Parameter Expansions, Iteration, and Averaging Methods.* World Scientific.
[7]. **Nayfeh, A.H., & Mook, D.T.** (2008). *Nonlinear Oscillations.* Wiley-VCH.
[8]. **Press, W.H., Teukolsky, S.A., Vetterling, W.T., & Flannery, B.P.** (2007). *Numerical Recipes: The Art of Scientific Computing* (3rd ed.). Cambridge University Press.